Electronic Supplementary Information

Configurationally Constrained Crystallization of Brush Polymers with Polyethylene Oxide Side Chains

Huilou Sun[1], Duk Man Yu[2], Shaowei Shi[1], Qingqing Yuan[3], So Fujinami[6], Xiaoli Sun[1], Dong Wang[3], Thomas P. Russell[1,2,4,5*]*

1. Beijing Advanced Innovation Center for Soft Matter Science and Engineering, Beijing University of Chemical Technology, Beijing 100029, China

2. Polymer Science and Engineering Department, University of Massachusetts, Amherst, Massachusetts 01003, USA

3. State Key Laboratory of Organic−Inorganic Composites, Beijing University of Chemical Technology, Beijing 100029, China

4. Materials Sciences Division, Lawrence Berkeley National Laboratory, 1 Cyclotron Road, Berkeley, California 94720, USA

5. Advanced Institute of Materials Research (AIMR), Tohoku University, 2-1-1 Katahira, Aoba, Sendai 980-8577, Japan

6. RIKEN SPring-8 Center, 1-1-1 Kouto, Sayo-cho, Sayo-gun, Hyogo 679-5148, Japan

* Corresponding author: e-mail: shisw@mail.buct.edu.cn; russell@mail.pse.umass.edu

Table S1. Kinetics parameters of homo-PEO, NB-PEO and brush-PEO during isothermal crystallization.

M_n	T_C (K)	n	K	$t_{1/2}$ (min)	t_{max} (min)	G (min^{-1})
homo-PEO	309	2.1	14.45	0.24	0.21	4.17
(M_n≈6K)	311	2.1	12.02	0.26	0.22	3.85
	313	2.0	5.75	0.35	0.29	2.86
	315	2.0	2.57	0.52	0.44	1.92
homo-PEO	309	2.1	4.68	0.40	0.35	2.50
(M_n≈3K)	311	2.3	2.29	0.59	0.54	1.69
	313	3.0	2.45	0.66	0.65	1.51
	315	2.0	0.50	1.18	1	0.56
NB-PEO	309	1.8	8.51	0.25	0.19	4
(M_n≈6K)	311	1.9	4.99	0.35	0.29	2.86
	313	1.8	2.45	0.50	0.39	2
	315	1.6	0.91	0.84	0.57	1.19
NB-PEO	309	1.9	9.51	0.25	0.21	4

(M_n≈3K)	311	1.5	2.81	0.39	0.24	2.56
	313	2.0	1.26	0.74	0.63	1.35
	315	2.6	0.09	2.19	2.09	0.46
brush-PEO	309	2.1	7.76	0.32	0.28	3.13
(SM_n≈6K)	311	1.8	5.50	0.33	0.25	3.03
	313	2.0	2.34	0.54	0.46	1.85
	315	2.1	0.52	1.15	1.00	0.87
brush-PEO	309	1.9	7.76	0.28	0.23	3.57
(SM_n≈3K)	311	2.0	3.24	0.46	0.39	2.17
	313	2.0	0.42	1.28	1.09	0.78
	315	2.6	0.02	3.91	3.74	0.26

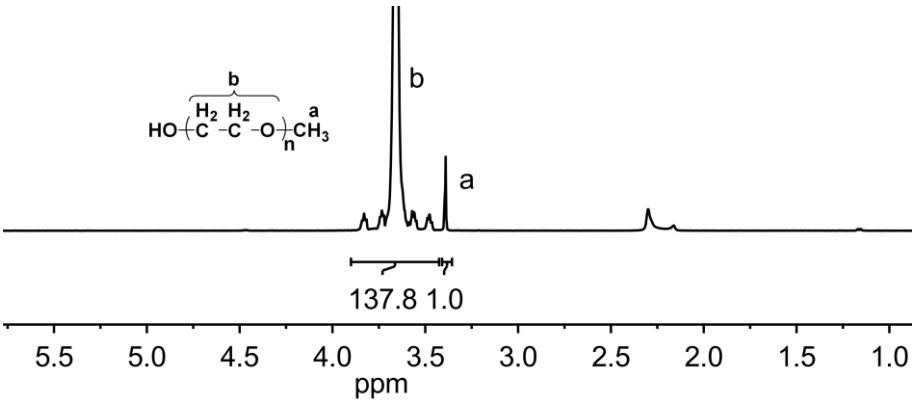

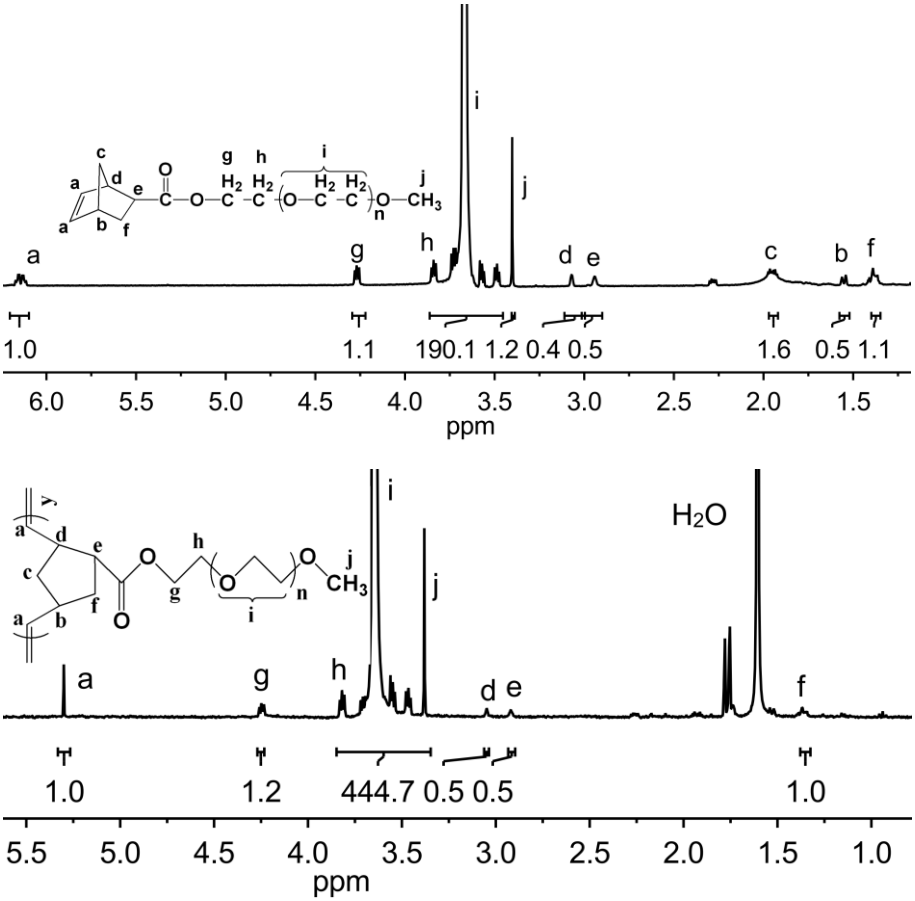

Figure S1. ^{1}H-NMR spectrum of homo-PEO, NB-PEO and brush-PEO.

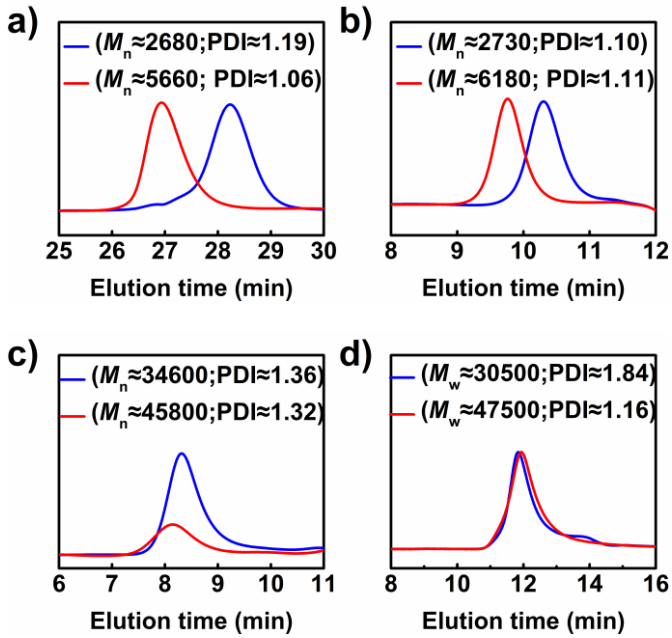

Figure S2. SEC traces of (a) homo-PEO, (b) NB-PEO, (c) brush-PEO. (d) SEC-MALS traces of brush-PEO.

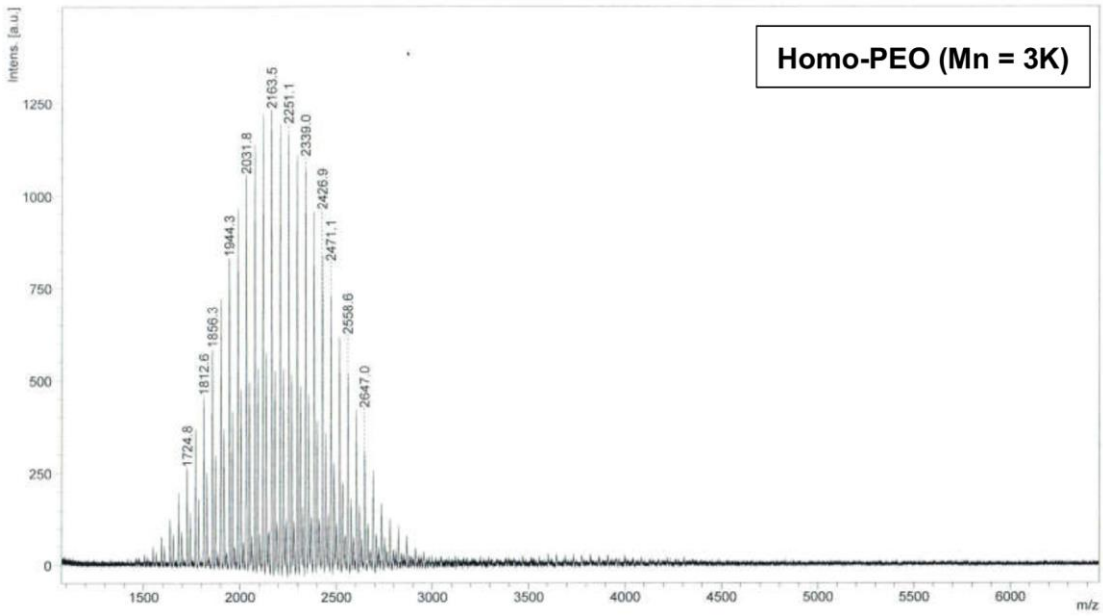
Homo-PEO (Mn = 3K)
Intens. [a.u.]
1250
1000
750
500
250
0
1724.8
1812.6
1856.3
1944.3
2031.8
2163.5
2251.1
2339.0
2426.9
2471.1
2558.6
2647.0
1500
2000
2500
3000
3500
4000
4500
5000
5500
6000
m/z

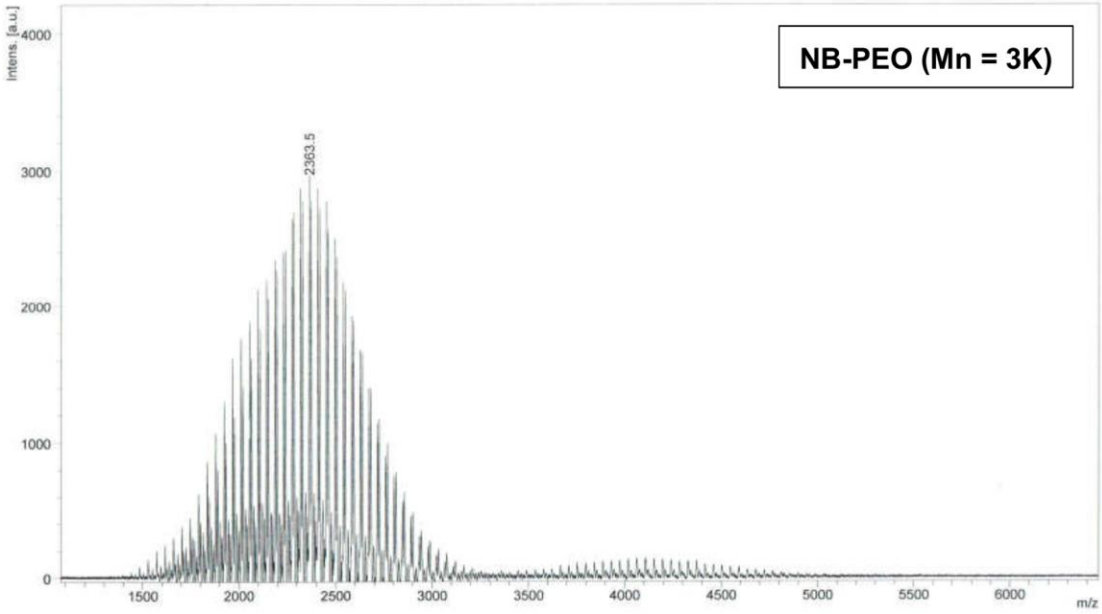
NB-PEO (Mn = 3K)
Intens. [a.u.]
4000
3000
2000
1000
0
2363.5
1500
2000
2500
3000
3500
4000
4500
5000
5500
6000
m/z

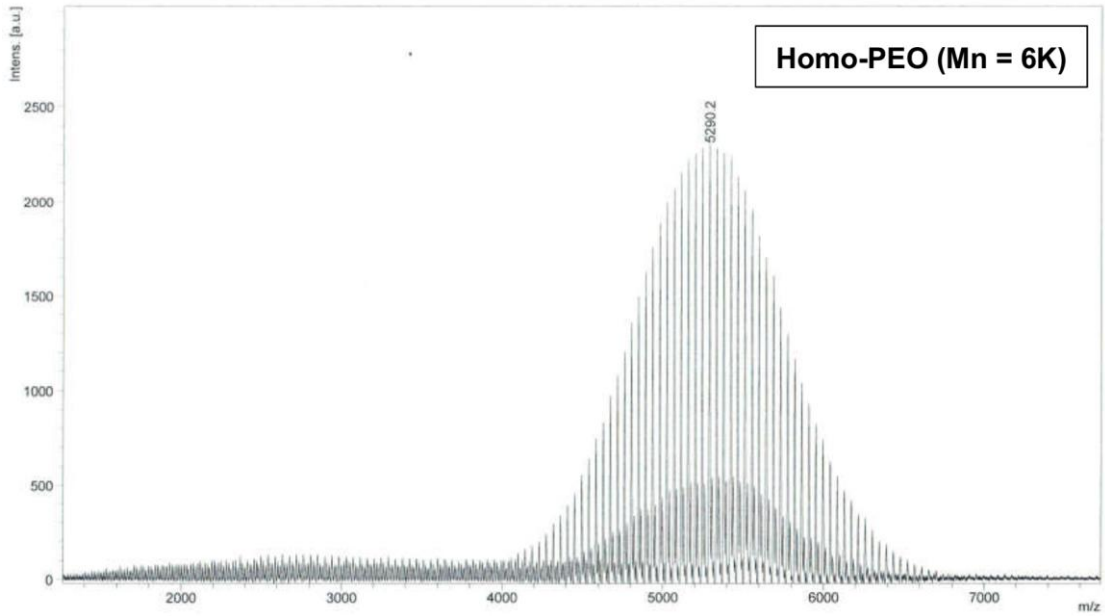

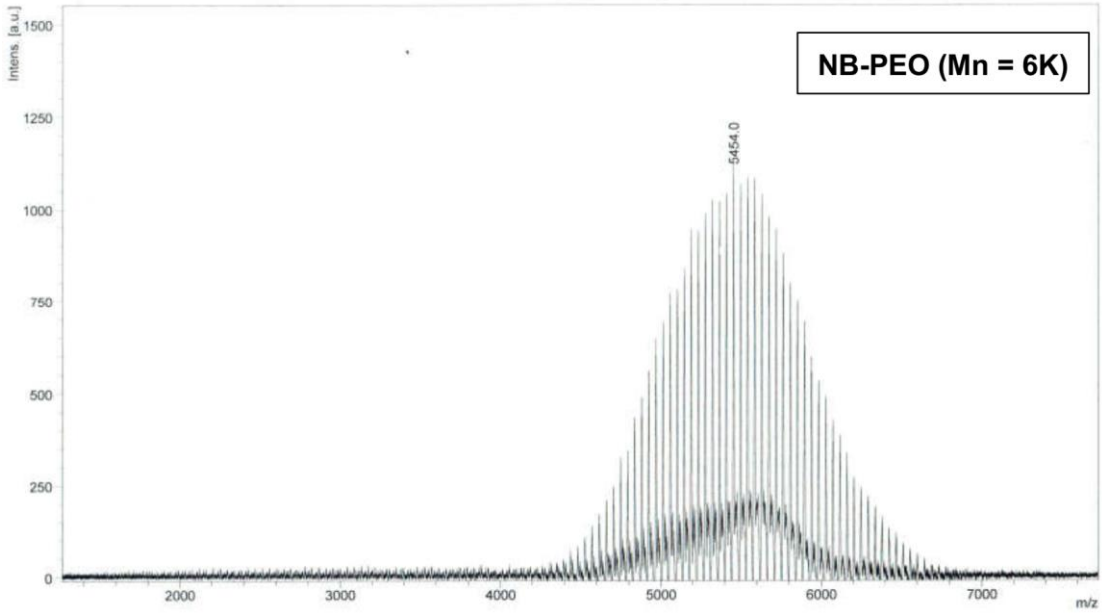

Figure S3. Mass spectrometry of homo-PEO and NB-PEO.

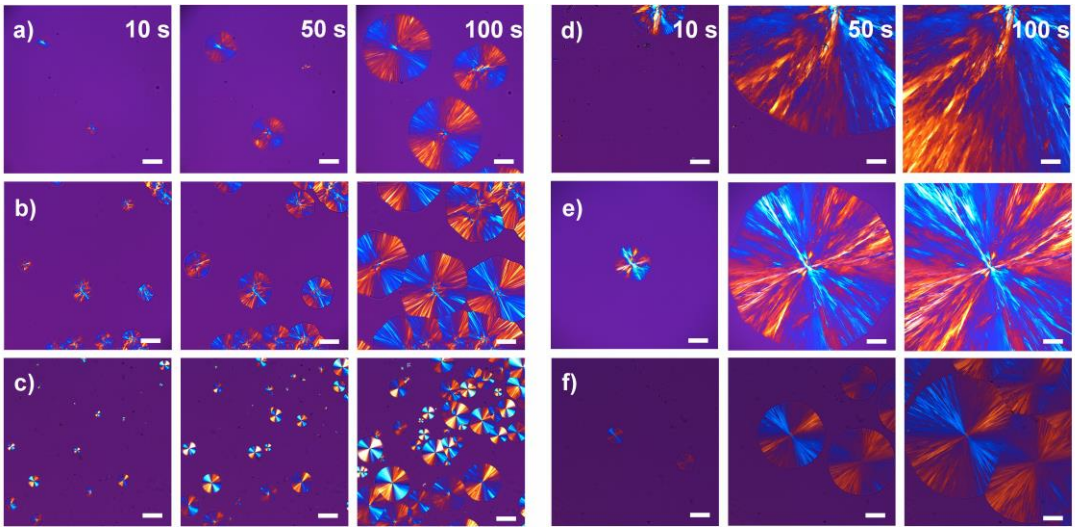

Figure S4. Polarized optical micrographs of homo-PEO (a. $M_n \approx 3K$; d. $M_n \approx 6K$), NB-PEO (b. $M_n \approx 3K$; e. $M_n \approx 6K$), and brush-PEO (c. S$M_n \approx 3K$; f. S$M_n \approx 6K$) crystallized at 40 °C for 10 s, 50 s, and 100 s respectively. Scale bar = 100 μm.

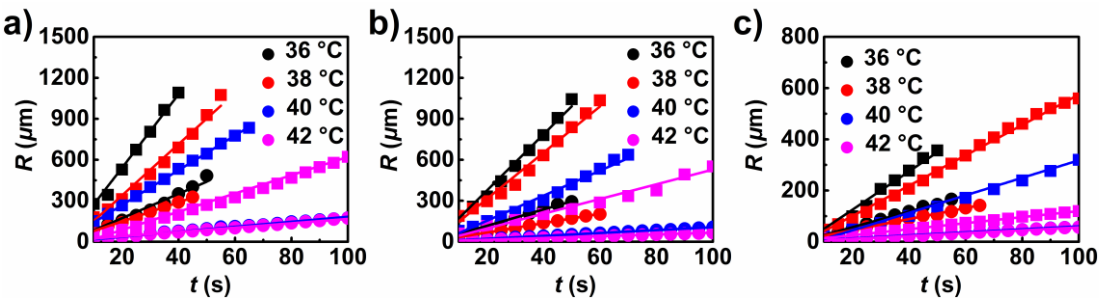

Figure S5. Variation in the spherulite radius R with the crystallization time for (a) homo-PEO, (b) NB-PEO and (c) brush-PEO measured at different crystallization temperature. The squares represent a molecular weight of 6K and the circle represents a molecular weight of 3K.

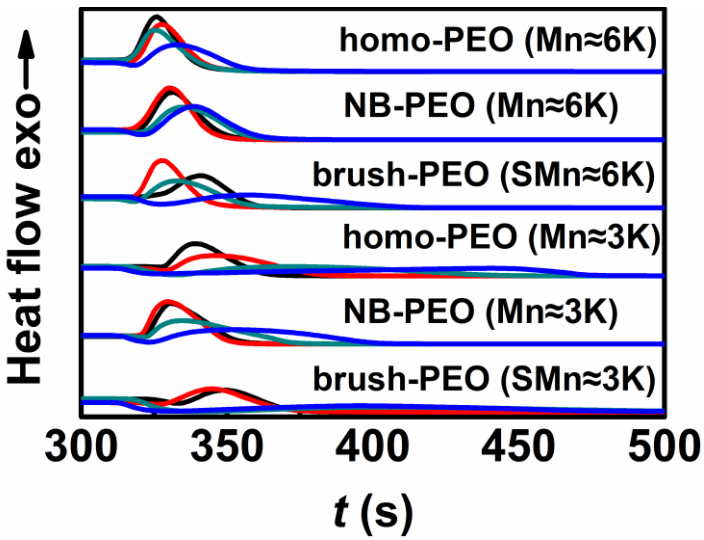

Figure S6. DSC curves for polymers during isothermal crystallization at different crystallization temperature 36 °C (black curve), 38 °C (red curve), 40 °C (green curve) and 42 °C (blue curve).

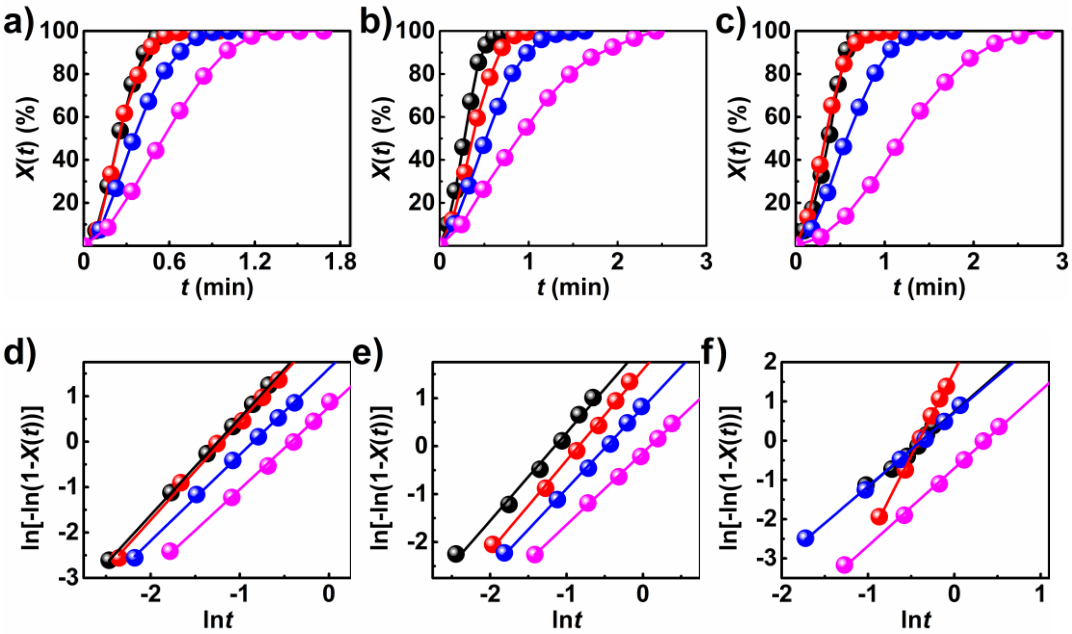

Figure S7. Isothermal crystallization $X(t)$-t curves and Avrami curves of (a, d) homo-PEO, $M_n \approx$ 6K, (b, e) NB-PEO $M_n \approx$ 6K and (c, f) brush-PEO, S$M_n \approx$ 6K under different crystallization temperature 36 °C (black curve), 38 °C (red curve), 40 °C (blue curve) and 42 °C (purple curve).

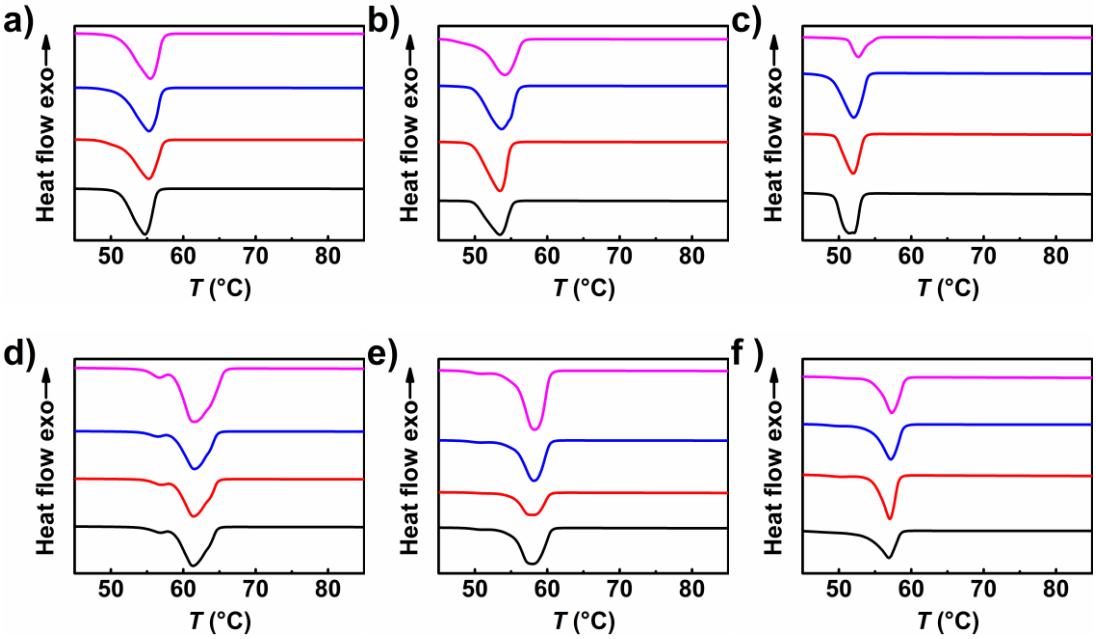

Figure S8. DSC heating curves of (a) homo-PEO, $M_n \approx$ 3K, (b) NB-PEO, $M_n \approx$ 3K, (c) brush-PEO, S$M_n \approx$ 3K, (d) homo-PEO, $M_n \approx$ 6K, (e) NB-PEO, $M_n \approx$ 6K, (f) brush-PEO, S$M_n \approx$ 6K crystallized at different crystallization temperature 36 °C (black curve), 38 °C (red curve), 40 °C (blue curve) and 42 °C (purple curve).

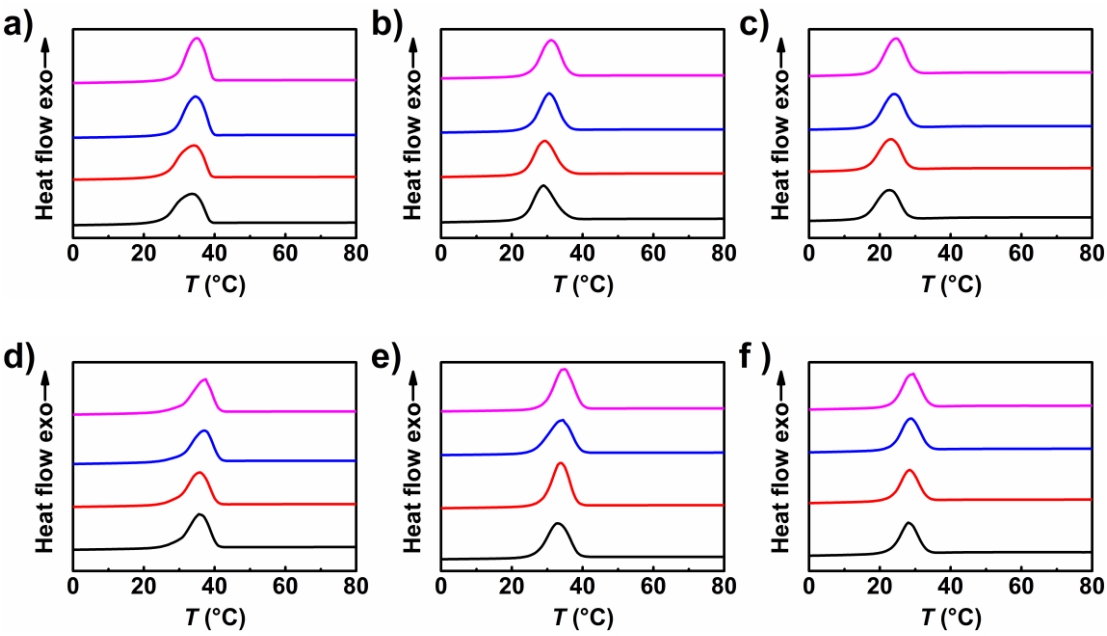

Figure S9. DSC cooling curves of (a) homo-PEO, $M_n \approx$ 3K, (b) NB-PEO, $M_n \approx$ 3K, (c) brush-PEO, S$M_n \approx$ 3K, (d) homo-PEO, $M_n \approx$ 6K, (e) NB-PEO, $M_n \approx$ 6K, (f) brush-PEO, S$M_n \approx$ 6K crystallized at different crystallization temperature 36 °C (black curve), 38 °C (red curve), 40 °C (blue curve) and 42 °C (purple curve).

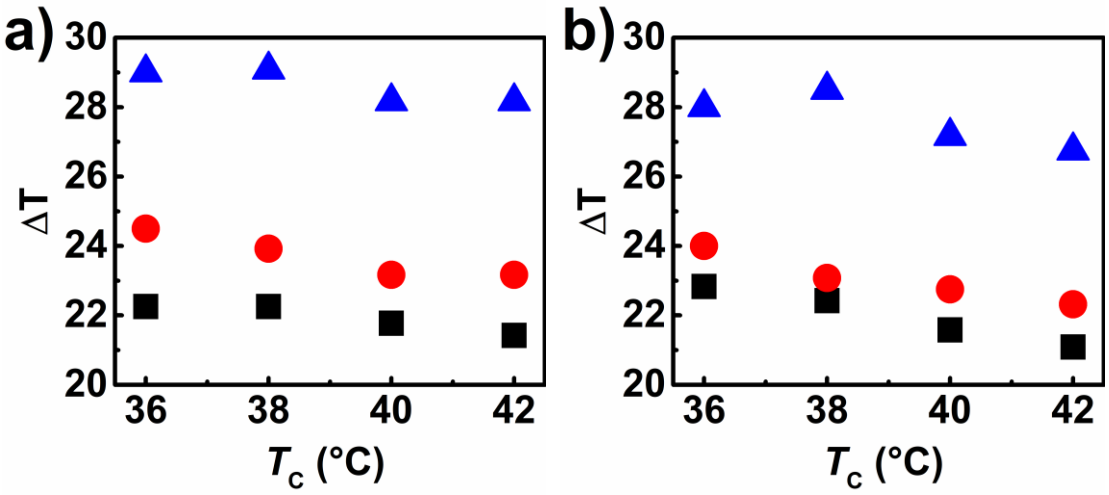

Figure S10. Supercooling of homo-PEO (black square), NB-PEO (red circle) and brush-PEO (blue triangle) after isothermal crystallization at different temperatures. (a) $M_n \approx 3$K, S$M_n \approx 3$K; (b) $M_n \approx 6$K, S$M_n \approx 6$K.

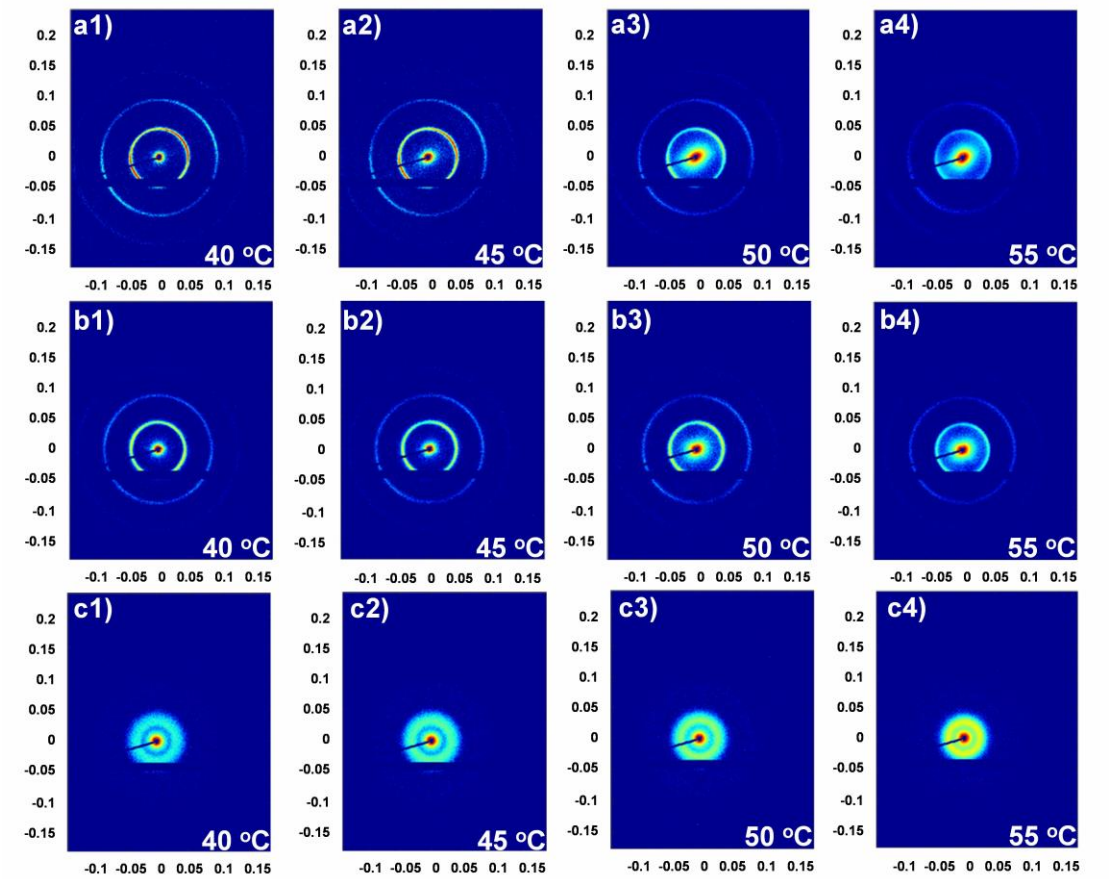

Figure S11. Representative 2D SAXS patterns for (a1-a4) homo-PEO, $M_n \approx 3$K, (b1-b4) NB-PEO, $M_n \approx 3$K and (c1-c4) brush-PEO, S$M_n \approx 3$K at different annealing temperatures.

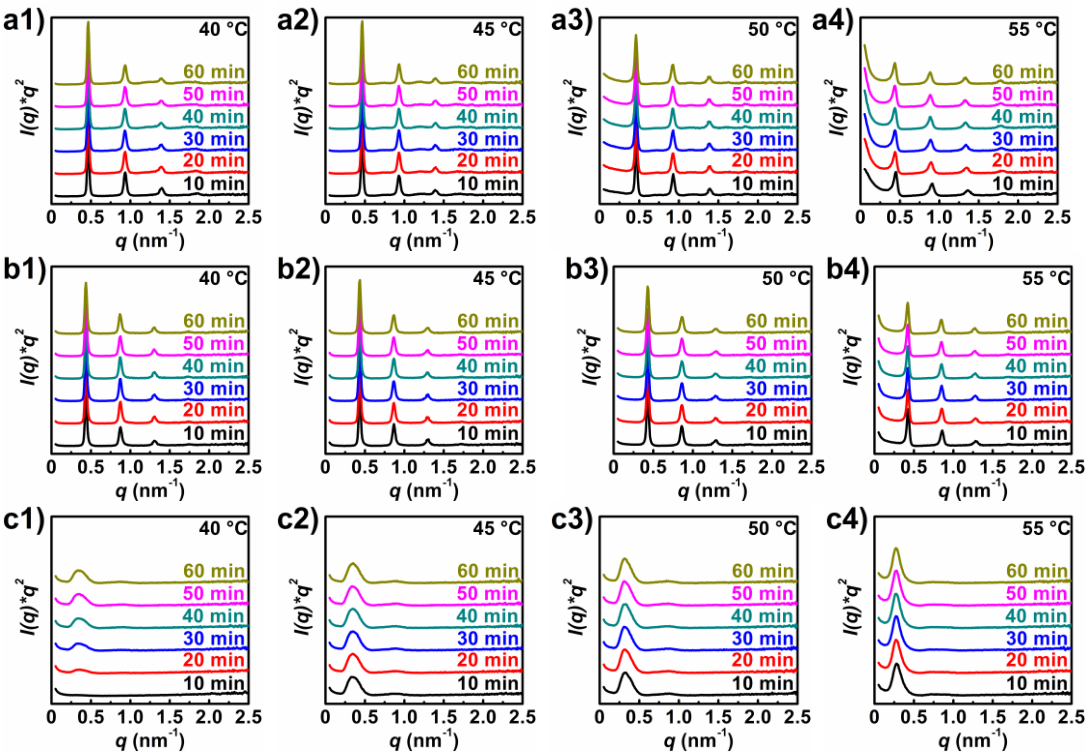

Figure S12. Lorentz-corrected SAXS profiles of (a1-a4) homo-PEO, $M_n \approx 3$K, (b1-b4) NB-PEO, $M_n \approx 3$K and (c1-c4) brush-PEO, S$M_n \approx 3$K at different annealing temperatures.

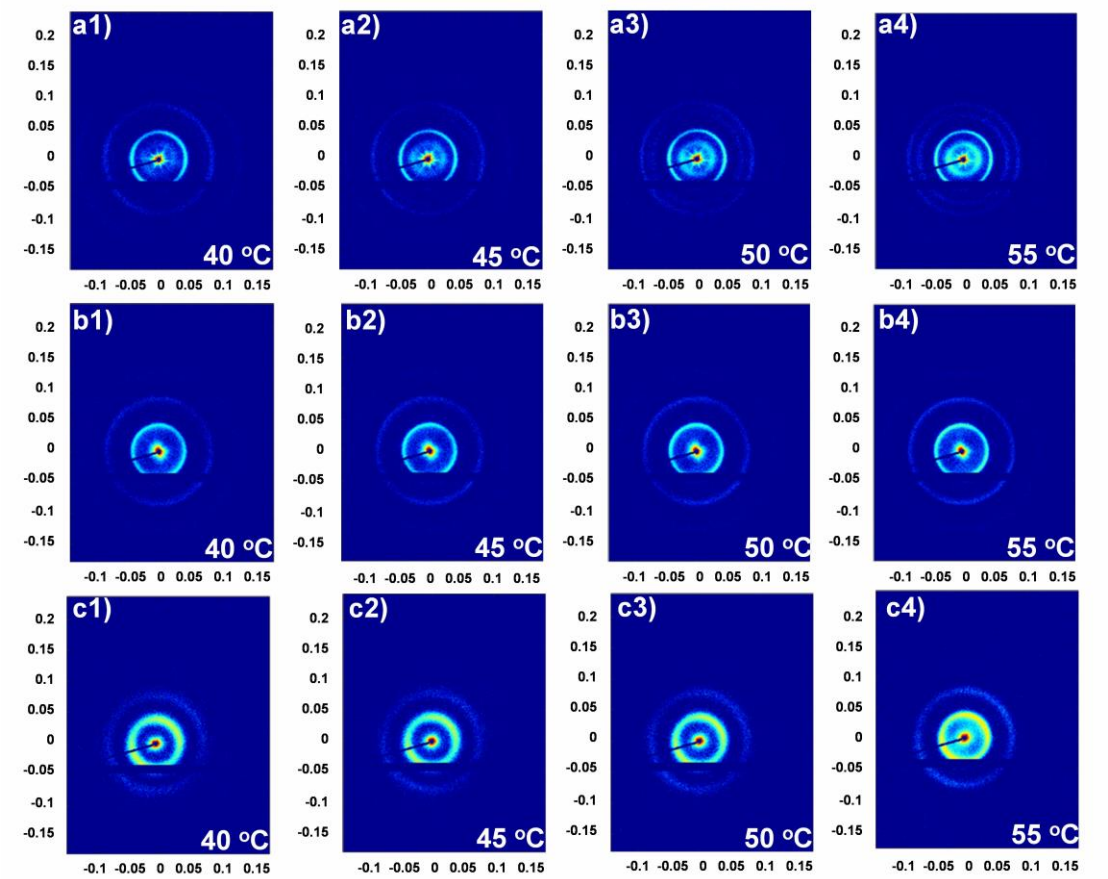

Figure S13. Representative 2D SAXS patterns for (a1-a4) homo-PEO, $M_n \approx 6K$, (b1-b4) NB-PEO, $M_n \approx 6K$ and (c1-c4) brush-PEO S$M_n \approx 6K$ at different annealing temperatures.

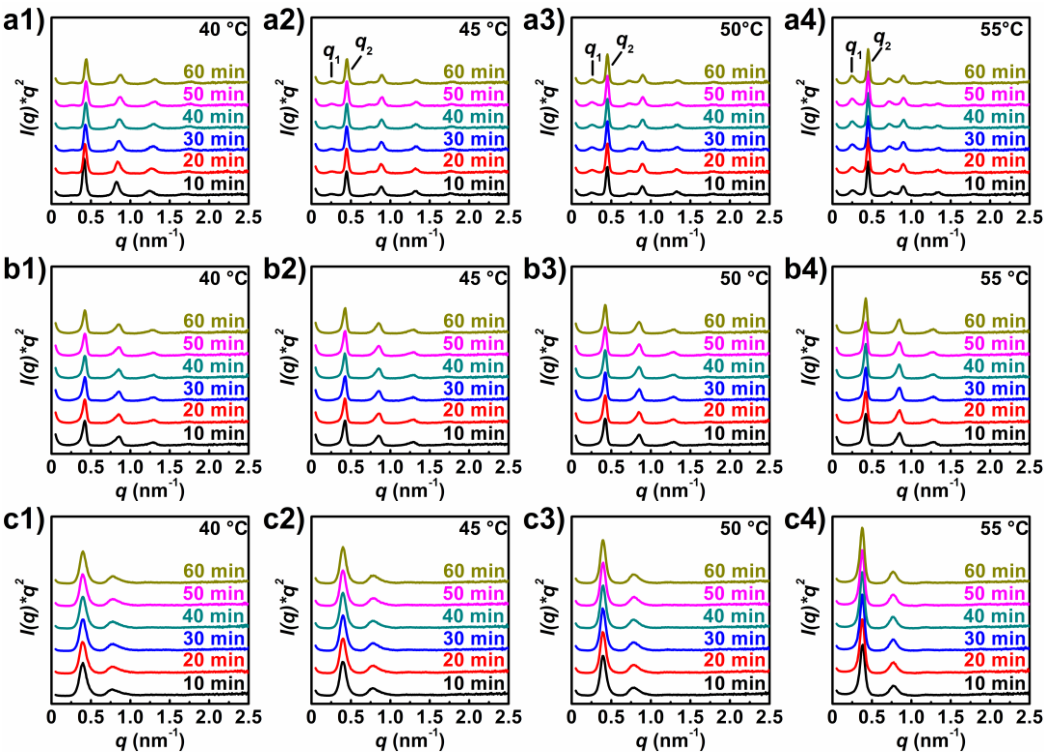

Figure S14. Lorentz-corrected SAXS profiles of (a1-a4) homo-PEO, $M_n \approx 6K$, (b1-b4) NB-PEO, $M_n \approx 6K$ and (c1-c4) brush-PEO, S$M_n \approx 6K$ at different annealing temperatures.